Compound Metacurl Antenna With C- and N-Type Metaatoms

HISAMATSU NAKANO[1], **(Life Fellow, IEEE), TOMOKI ABE**[1], **(Member, IEEE),**
AMIT MEHTA[2], **(Senior Member, IEEE), AND**
JUNJI YAMAUCHI[1], **(Life Fellow, IEEE)**
[1]Department of Science and Engineering, Hosei University, Tokyo 184-8584, Japan
[2]College of Engineering, Swansea University, Swansea SA1 8EN, U.K.

Corresponding author: Hisamatsu Nakano (hymat@hosei.ac.jp)

ABSTRACT A metacurl antenna made of C-type metaatoms (forming a C-type metaline), called the C-metacurl antenna, is investigated. The investigation reveals that the gain for a left-handed circularly polarized wave, LHCP gain, has a maximum value at frequency f_{LH} and the gain for a right-handed circularly polarized wave, RHCP gain, has a maximum value at different frequency f_{RH}, where the maximum LHCP gain is smaller than the maximum RHCP gain. Subsequently, a different metaatom that forms the unit cell of an N-type metaline, called the N-type metaatom, is investigated. It is found that the radiation from the N-type metaatom is LHCP. This infers that the maximum LHCP gain for the C-metacurl antenna will increase when some C-type metaatoms are replaced by N-type metaatoms. Based on this inference, a novel metacurl antenna composed of C-type metaatoms and N-type metaatoms, called the compound metacurl antenna, is analyzed. The analysis reveals that replacement with an appropriate number of N-type metaatoms increases the maximum LHCP gain, resulting in a balancing of LHCP gain and RHCP gain. The antenna characteristics under such a gain-balanced situation, including the radiation pattern, axial ratio, and input characteristic (VSWR), are also discussed.

INDEX TERMS Metacurl antennas, metaatoms, circularly polarized wave, gain.

I. INTRODUCTION

A helical antenna backed by a conducting ground plane radiates a circularly polarized (CP) wave in the antenna axis direction normal to the ground plane when the circumference of the helical arm is approximately one wavelength [1]–[3]. This radiation is called end fire mode radiation or axial mode radiation. The inventor of the end fire mode helical antenna, J. D. Kraus, qualitatively explained the radiation characteristics in 1947. Later, in 1978, the authors showed quantitative analysis results based on an integral equation [4]–[6], which is solved using the method of moments [7], [8]. The qualitative and quantitative results have revealed that the rotational sense of the CP wave from the end fire mode helical antenna is either right-handed (RH) or left-handed (LH), subject to the winding sense of the helical arm.

A two-arm spiral antenna backed by a conducting plate is also a CP antenna [9]–[13]. Conventionally, the two arms are excited with equal amplitude and a phase difference of 180 degrees. The radiation mechanism of the spiral antenna has been qualitatively explained using Kaiser's electrical current band theory [9]. As with the radiation characteristics for the helical antenna, those for the spiral antenna have also been rigorously analyzed using the integral equation in [14]. It is found that the CP wave from the spiral antenna has either an LH or an RH rotation, subject to the winding sense of the spiral arms.

A curl antenna [15] shown in Fig. 1(a) is a first modification of the two-arm spiral antenna, where the number of arms is reduced to one and the number of spiral turns is also reduced to less than two. The curl antenna arm is shorter than the spiral antenna arm; however, it radiates a CP wave in the quasi-broadside direction normal to the curl antenna plane [15]–[19]. This is attributed to the fact that a traveling wave with smooth decay toward the arm end is distributed
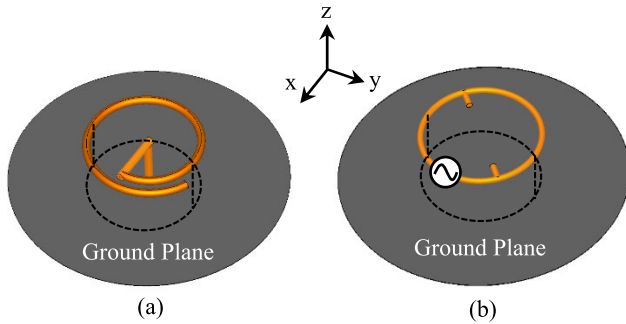
FIGURE 1. (a) CP curl antenna. (b) CP loop antenna.

along the curled arm. The CP wave generated by the traveling wave has either an LH rotation or an RH rotation, as with the helical and spiral antennas. Note that the curl arm has an open end (no resistive load), as with the spiral antenna arm and the end fire mode helical antenna arm.

As opposed to curl antennas [15]–[19], a loop antenna has a closed arm shape. A standing wave current exists along the loop and hence the loop radiates a linearly polarized (LP) wave in the z-direction normal to the loop plane when the loop circumference is one wavelength [20], [21]. It has been shown that the standing wave can be transformed into a traveling wave when perturbation elements are added to the loop, as shown in Fig. 1(b) [22]. As a result, the initial LP radiation wave is changed into a CP radiation wave. The CP wave from the loop antenna has either an LH rotation or an RH rotation, depending on the location of the perturbation elements.

As described above, conventional CP helical, spiral, curl, and loop antennas have a *single* rotational sense (either an LH rotation or an RH rotation), when the feed is fixed. This is due to the fact that the current on these antennas has a positive propagation phase constant: $\beta > 0$. Hence, the phase progression along an antenna arm across a small length of Δs, denoted as $-\beta \Delta s$, is negative. In other words, the current has a regressive phase.

Recently, a CP curl antenna that differs from conventional curl antennas has been proposed [23]. This curl antenna is called a metamaterial curl antenna or a *metacurl antenna*, whose antenna arm is made of a C-type metamaterial line, which has the same operating mechanism as that for a composite right- and left-handed (CRLH) transmission line [24]–[26].

The metacurl antenna works as a leaky wave antenna with propagation phase constant $\beta < 0$ at frequencies below a specific frequency, f_T, and $\beta > 0$ at frequencies above f_T. Therefore, the metacurl works as a dual-band counter CP antenna, *i.e.*, if the metacurl radiates a left-handed circularly polarized (LHCP) wave at frequencies below f_T, then it radiates a right-handed circularly polarized (RHCP) wave at frequencies above f_T; conversely, if it radiates an RHCP wave at frequencies below f_T, then it radiates an LHCP wave at frequencies above f_T. Note that the CP metacurl antenna has

a small antenna height; it is on the order of $\lambda/100$, with λ being the free-space wavelength at the design frequency, unlike the $\lambda/4$ height of representative/conventional loop antennas.

In accordance with the rotational sense of the metacurl antenna, either the gain for the LHCP wave (LHCP gain) or the gain for the RHCP wave (RHCP gain) is dominant across each of the two frequency bands. However, the maximum LHCP gain and the maximum RHCP gain are not equal in value [27]. This difference in maximum gain values has limited the fields of application for the metacurl antenna. If a pair of dual-band counter CP antennas with different gains are used as a transmitting antenna and a receiving antenna, the receiving power levels of LHCP and RHCP waves are different. In this case, a post-processing circuit connected to the receiving antenna requires an additional amplifier to enhance the small power level of the LHCP wave or RHCP wave. This complicates the antenna fabrication and assembly.

One solution to resolving the unequal gains is to use a parasitic loop [28] above the metacurl antenna. However, this creates a disadvantage in that the attached parasitic loop increases the height of the total antenna system, although the metacurl antenna itself has the advantage of a low-profile structure. In addition, a two-layer structure composed of the metacurl and the parasitic loop complicates antenna assembly.

This paper presents an innovative CP metacurl antenna that has equal maximum gains in two different frequency bands below and above f_T, where the metacurl is printed on a single substrate to maintain its inherent low-profile antenna structure. This innovative antenna is called the *compound metacurl antenna*.

Six sections constitute this paper. In Section II, two straight metalines are analyzed. These metalines are called the C-type and N-type metalines. The former and latter radiate an LP wave and a CP wave, respectively. In Section III, the issue of unequal gains for a conventional dual-band counter CP metacurl antenna made of a curved C-type metaline is clarified. In Section IV, the radiation behavior for an N-type metaatom is clarified. Subsequently, an innovative compound metacurl antenna composed of C- and N-type metalines (metaatoms) is proposed and analyzed for equalizing the gains. The resulting equal gain values are confirmed by demonstrating agreement with the experimental results in Section V. Other antenna characteristics, including the radiation pattern, axial ratio, and VSWR, are also discussed. Section VI summarizes the results obtained in this paper. Note that the numerical analysis in this paper is performed using an electromagnetic field solver based on the finite element method [29].

II. C- AND N-TYPE METALINES
A C-type metamaterial line and an N-type metamaterial line are prepared for fabricating the compound metacurl antenna. These lines, both having width w, are shown in Figs. 2(a) and (b).
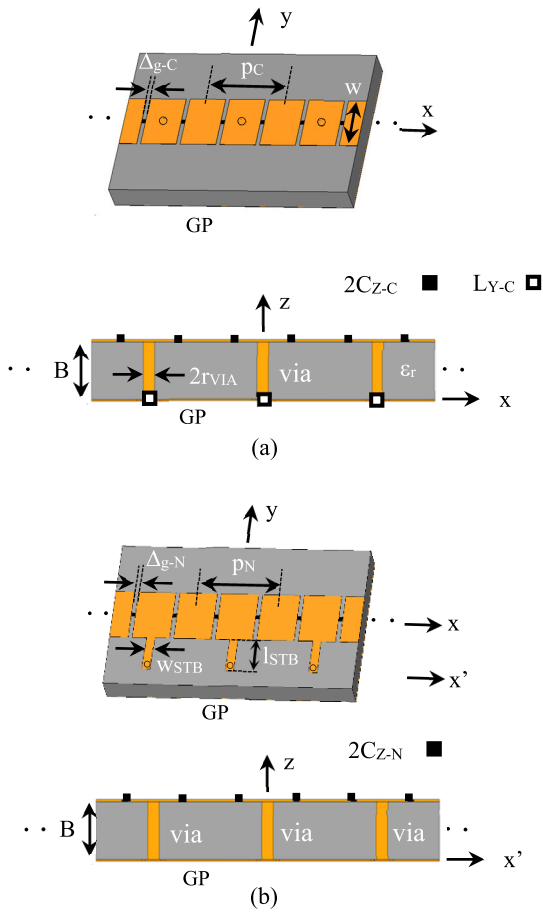
FIGURE 2. Metamaterial lines (metalines). (a) Perspective and side views of C-type metaline. (b) Perspective and side views of N-type metaline.

FIGURE 3. Dispersion diagram. (a) C-type metaline. (b) N-type metaline.

TABLE 1. Parameters.

Symbol	Value	Symbol	Value
B	1.6 mm	w_{STB}	1.2 mm
w	4.4 mm	l_{STB}	6.0 mm
ε_r	2.6	r_{VIA}	0.5 mm
$p_C = p_N$	10.0 mm	$2C_{Z-C} = 2C_{Z-N}$	1.6 pF
$\Delta_{g-C} = \Delta_{g-N}$	0.5 mm	L_{Y-C}	1.8 nH

The C-type metaline is made of repeated subwavelength strips, where a section of length p_C is designated as the C-type metaatom. Neighboring subwavelength strips, which are separated by gap Δ_{g-C}, are connected through a chip capacitor, $2C_{Z-C}$. A conducting pin of radius r_{VIA} is extended from the central strip of the C-type metaatom and connected to the ground plane (GP) through a chip inductor, L_{Y-C}. The C-type metaline realizes a CRLH transmission line [24].

The N-type metaline is also made of repeated subwavelength strips, where a section of length p_N ($= p_C$) is designated as the N-type metaatom. Neighboring subwavelength strips, which are separated by gap Δ_{g-N} ($= \Delta_{g-C}$), are connected through a chip capacitor, $2C_{Z-N}$ ($= 2C_{Z-C}$). A stub is extended from the N-type metaatom in the negative y-direction and shorted to the ground plane. The width and length of the stub are denoted as w_{STB} and l_{STB}, respectively.

Fig. 3 shows the dispersion diagram for the C- and N-type metalines, where β is the propagation phase constant along each line and k_0 is the phase constant in free space. The parameters used for Fig. 3 are summarized in Table 1. The N-type metaline is designed to have dispersion that is as similar as possible to the C-type metaline, where transition
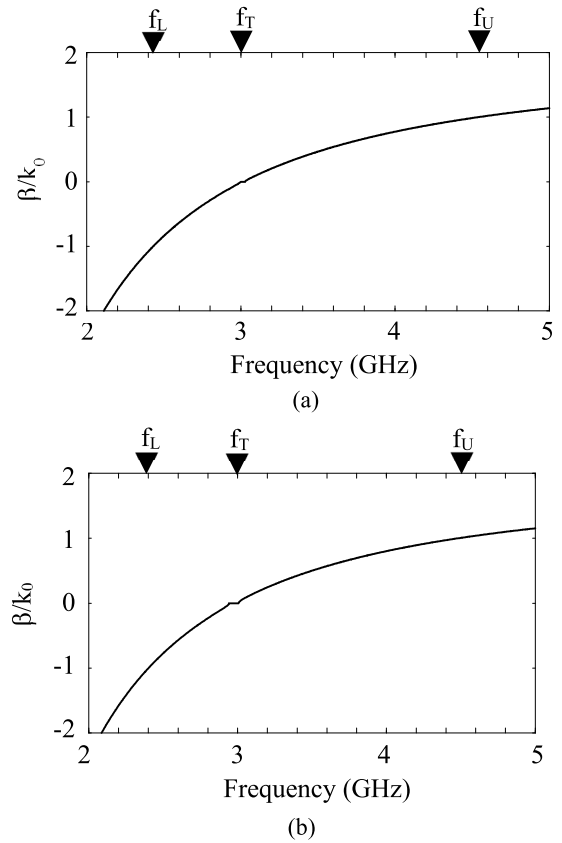
frequency f_T is set to be 3 GHz. The lower- and upper-edge frequencies for a fast wave are denoted as f_L and f_U, respectively.

Based on Fig. 3, the guided wavelength, λ_g, as a function of frequency f is obtained and shown in Fig. 4. It is found that the guided wavelength has the same value at two frequencies; one is located within the negative β region and the other is located within the positive β region.

III. METACURL ANTENNA USING A C-TYPE METALINE (C-METACURL ANTENNA)

A. CONFIGURATION AND RADIATION MECHANISM

Fig. 5 shows a curl antenna made of the C-type metaline whose parameters are shown in Table 1. This structure is designated as the C-metacurl antenna. Point F is the feed point, where the inner conductor of a coaxial feed line is
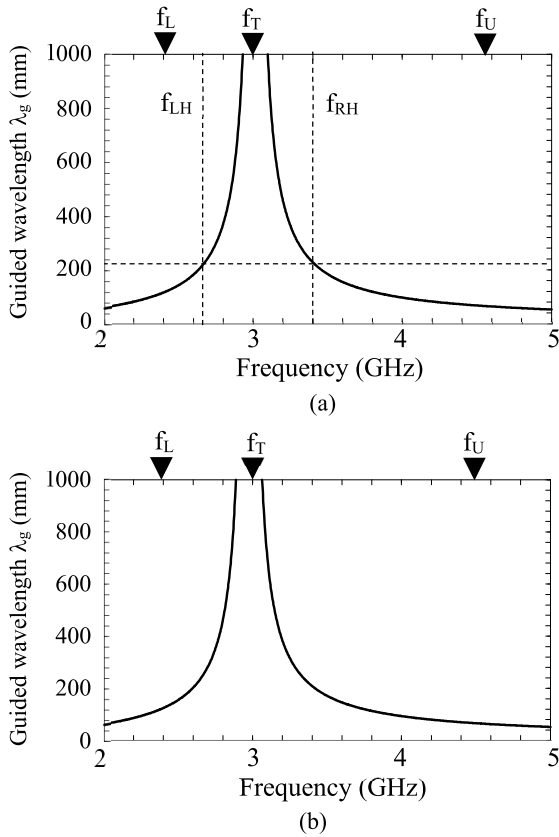
FIGURE 4. Guided wavelength λ_g. (a) C-type metaline. (b) N-type metaline.
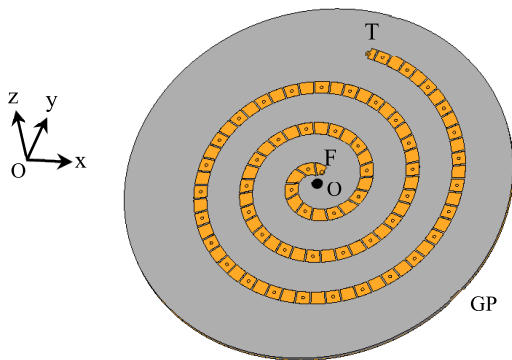

FIGURE 5. C-metacurl antenna made of numerous C-type metaatoms.

connected. Point T is the terminal point, which is shorted to the ground plane through a resistive load (Bloch impedance of 50 ohms). The radial distance from the coordinate origin O to a point on the curled arm is defined by a function of $r_{curl} = a_{curl}\phi_{wind}$, where a_{curl} is a growth constant and ϕ_{wind} is an arm winding angle. Values of $a_{curl} = 2.45$ mm/rad and 0.5π rad $\leq \phi_{wind} \leq 6.5\pi$ rad are used in this paper. As a result, the curled arm circumference (defined as $2\pi r_{curl-max}$ with $r_{curl-max}$ being maximum r_{curl}) is approximately 314 mm. Note that this circumference is chosen such that it is larger than a circular active region of one guided wavelength ($1\lambda_g$) circumference for CP axial beam radiation, as seen from the
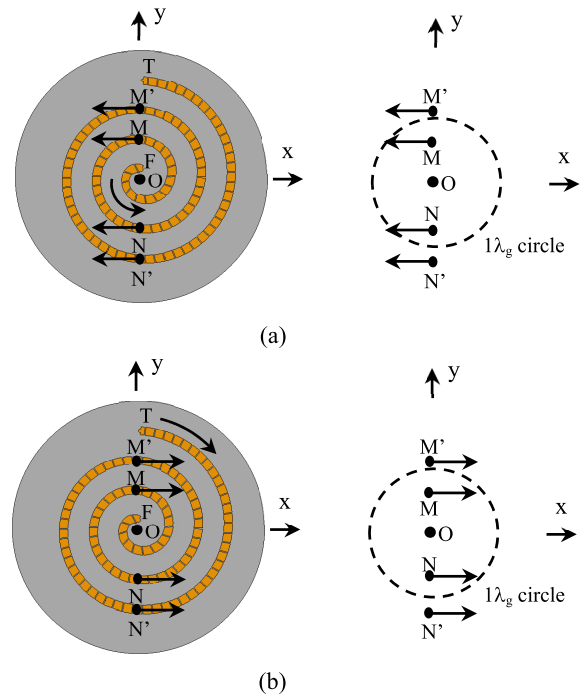

FIGURE 6. Current bands. (a) For positive β. (b) For negative β.

following paragraphs. In other words, the antenna is designed to have a size that includes the $1\lambda_g$ circular active region.

The radiation from the metacurl antenna is qualitatively explained using the current along the curled arm, which flows in a traveling wave fashion by virtue of the Bloch impedance. Fig. 6 shows two cases of the current, where the propagation phase constant β is positive in Fig. 6(a) and negative in Fig. 6(b).

Neighboring currents at points M and M' on the curled arm in Fig. 6(a) become in-phase when the length from point N to point M' along the curled arm at a certain frequency f_{RH} is half the guided wavelength ($\lambda_g/2$), resulting in creation of a current band [9], where points N and M are quasi-symmetric with respect to the antenna center point O, i.e., the radial distance r_{curl} at point $M \approx$ the radial distance r_{curl} at point N. Note that almost in-phase currents appear at points N and N', because the length from point M' to point N' along the curled arm is close to $\lambda_g/2$. Thus, these two current bands are created near a circle whose circumference on the antenna plane is approximately $1\lambda_g$ at a certain frequency of f_{RH} ($> f_T$), and these current bands rotate *counterclockwise* along a region near the $1\lambda_g$ circle with change in time t, resulting in generation of the maximum RHCP radiation in a direction near the positive z-axis at f_{RH}. (In this context, a region near the circle of $1\lambda_g$ circumference is called the active region for CP axial beam radiation). The antenna arm is not symmetric with respect to the z-axis and hence a very small deviation of the maximum RHCP radiation from the z-axis appears, as shown later.

The current flowing along a small curled arm length of Δs experiences a phase progression of $-\beta\Delta s$, which is negative
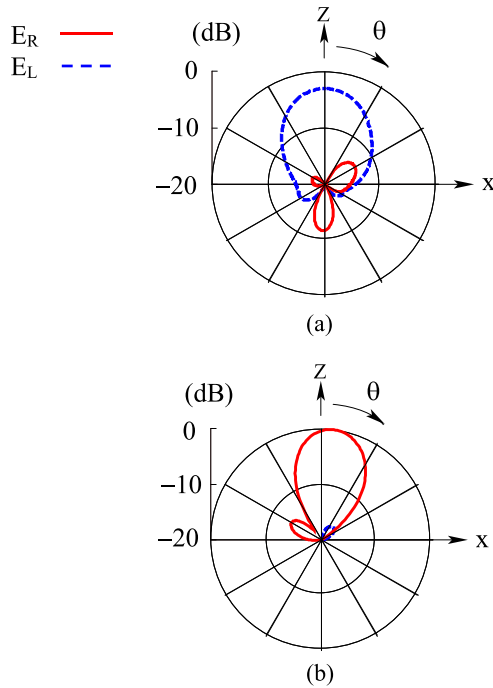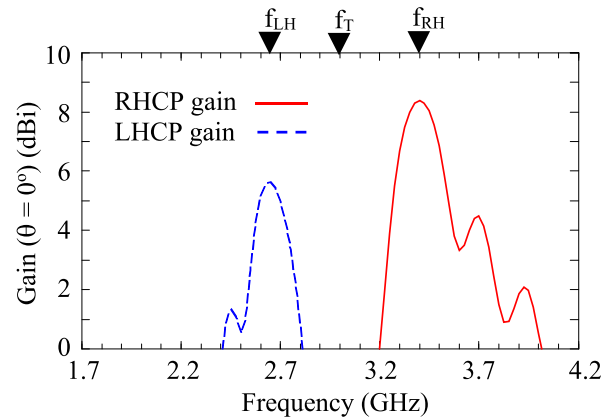
FIGURE 7. Radiation pattern for the C-metacurl antenna. (a) At f_{LH}, where the propagation phase constant β is negative. (b) At f_{RH}, where β is positive. Note that the radiation pattern is normalized to the maximum value at f_{RH}.

FIGURE 8. Frequency response of the gain for the C-metacurl antenna.

(regressive/delayed) in Fig. 6(a) due to positive β and is positive (progressive) in Fig. 6(b) due to negative β. The latter means that the current in Fig. 6(b) behaves as if it travels clockwise from ending point T to starting point F. Two *clockwise* current bands, which are opposed to the positive β case with respect to the rotational sense, are created on the active region of approximately $1\lambda_g$ at a certain frequency of f_{LH} ($< f_T$). These bands rotate on the $1\lambda_g$ active region and generate an LHCP wave with the maximum intensity appearing slightly off the positive z-axis.

B. RADIATION PATTERN AND GAIN
Fig. 7(a) shows the radiation pattern at 2.65 GHz, where the LHCP gain reaches the maximum. The E_L and E_R in this figure denote the LHCP wave and RHCP wave components of the radiation, respectively. It is found that the co-polarized radiation component E_L forms an axial beam and is slightly deviated from the z-axis due to the asymmetry of the antenna configuration with respect to the z-axis. Note that the frequency of 2.65 GHz is a frequency within the negative β region in Fig. 3(a) and labelled as f_{LH} based on the radiation mechanism described in subsection A.

The radiation pattern when the RHCP gain reaches the maximum at 3.4 GHz is shown in Fig. 7(b). The co-polarized radiation component E_R forms an axial beam. As with the radiation E_L at f_{LH} ($= 2.65$ GHz), the radiation component E_R at 3.4 GHz is slightly deviated from the z-axis. The frequency of 3.4 GHz is a frequency within the positive β region in Fig. 3(a). The fact revealed above allows us to label 3.4 GHz as f_{RH}.
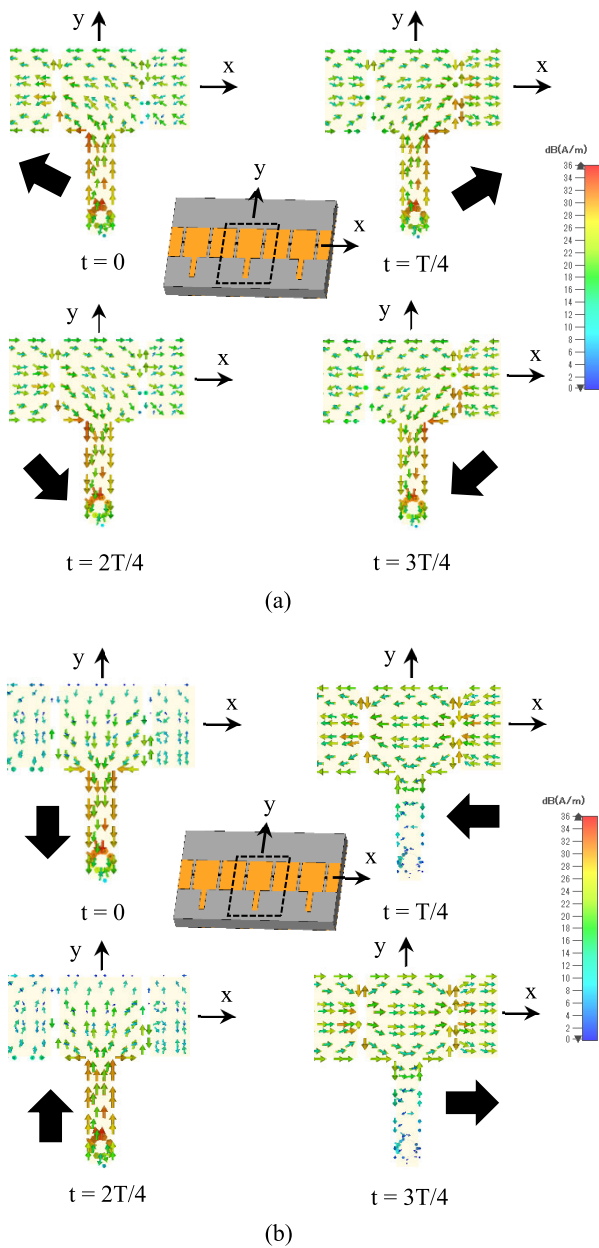
Using Fig. 4(a), it is found that the guided wavelength λ_g is 220 mm at f_{LH} and 216 mm at f_{RH}. These guided wavelengths are very close to each other; this means that LHCP radiation and RHCP radiation are generated from a common active region. Based on these guided wavelengths, the average circumference of the $1\lambda_g$-active region is estimated to be 218 mm, which is smaller than the antenna circumference $2\pi r_{curl-max}$ ($= 314$ mm), meeting the requirement for generating a CP axial beam.

Fig. 8 shows the gain for the C-metacurl antenna as a function of frequency. The LHCP gain is dominant at frequencies around f_{LH} ($= 2.65$ GHz) and the RHCP gain is dominant at frequencies around f_{RH} ($= 3.4$ GHz). A finding is that the LHCP gain and RHCP gain are unbalanced (not equal); the maximum LHCP gain is smaller than the maximum RHCP gain. This is attributed to the fact that the common $1\lambda_g$ active radiation region relative to the operating wavelength at f_{LH} is smaller than that at f_{RH}, i.e., $1\lambda_g/\lambda_{LH} < 1\lambda_g/\lambda_{RH}$ with λ_{LH} and λ_{RH} being the operating wavelengths (free-space wavelengths) at f_{LH} and f_{RH}, respectively. In other words, the *electrical* active radiation region at f_{LH} is smaller than that at f_{RH}. Thus, the gain at f_{LH} is smaller than the gain at f_{RH}.

IV. MODIFIED C-METACURL ANTENNA (COMPOUND METACURL ANTENNA)
Section III reveals the behavior for the radiation pattern and gain of a C-metacurl antenna. Before we control the gain for the C-metacurl antenna, we clarify the radiation from an N-type metaatom that is the unit element for the N-type metaline. Fig. 9 shows the change in the magnetic field vector above the N-type metaatom surface when time t is changed, where the frequency is fixed to be f_{LH} ($= 2.65$ GHz) in Fig. 9(a) and f_{RH} ($= 3.4$ GHz) in Fig. 9(b). It is revealed that the field vectors rotate clockwise at these two frequencies. This is the reason why the N-type metaline is an LHCP radiation element.
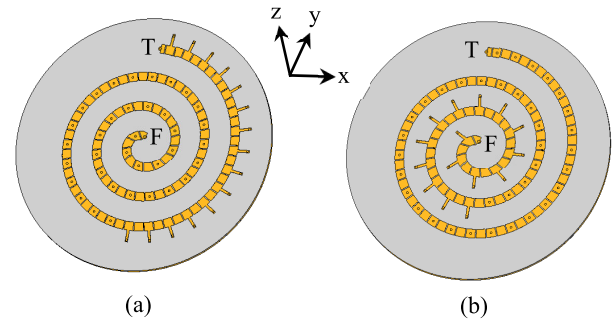
From the fact that the LHCP radiation is generated by the N-type metaatoms, it is inferred that the gain for the C-metacurl antenna will be controlled by replacing some C-type metaatoms by the N-type metaatoms, i.e., it is

FIGURE 10. Compound metacurl antennas. (a) Compound-T metacurl antenna. (b) Compound-F metacurl antenna.

The number of N-type metaatoms used for the replacement is denoted as N_N. Note that the total number of metaatoms for the compound metacurl antenna remains unchanged, which is 51 (which is the same as the number of C-type metaatoms used for the original C-metacurl antenna in Fig. 5).

Fig. 11(a) shows the frequency response of the gain for the compound-T metacurl antenna, where the number of N-type metaatoms, N_N, is used as a parameter. It is found that the LHCP gain and the RHCP gain have almost equal maximum values at $N_N = 15$. Similar investigation is performed for the compound-F metacurl antenna, as shown in Fig. 11(b). It is revealed that almost equal maximum gains are obtained at $N_N = 21$.

Comments are made here. The N-type metaatom does not act as an LHCP radiation element at f_{RH} (= 3.4 GHz). The reduction of the gain in the high frequency band is due to reduction in the number of C-type metaatoms. According to numerical analysis, increase in the number of N-type metaatoms, N_N, does not deteriorate the axial ratio at f_{RH} (see Fig. 18 in Appendix).

As inferred, the N-type metaatom can control the gain for the compound metacurl antenna. Based on this fact, we further investigate the radiation characteristics, focusing on the compound-T metacurl antenna as a representative of the two compound metacurl antennas. Note that fifteen N-type metaatoms that provide the equal maximum gains are used for the following discussion.

Fig. 12 shows the radiation patterns when the maximum LHCP gain at 2.7 GHz equals the maximum RHCP gain at 3.45 GHz. These frequencies are very close to f_{LH} (= 2.65 GHz) and f_{RH} (= 3.4 GHz), respectively. In other words, replacement by the N-type metaatoms does not significantly affect the frequencies for maximum LHCP and RHCP gains.

The input characteristic for the compound-T metacurl antenna in terms of the VSWR is presented in Fig. 13. It is found that the VSWR is less than 2 across the two 3-dB gain bandwidth regions, as desired. This is attributed to the fact that arm end T is terminated to the ground plane through a Bloch impedance (50 ohms), thereby reducing reflected currents from T toward starting point F.
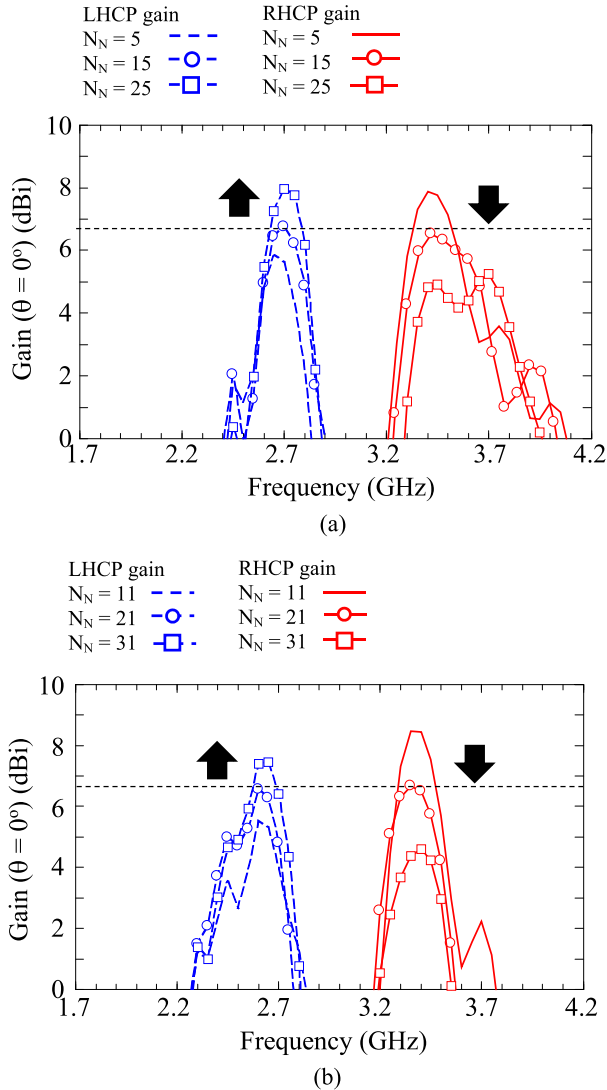

FIGURE 9. Magnetic field vectors above the surface of the N-type metaatom when time t is changed with periodicity T. (a) At frequency f_{LH} (< f_T). (b) At frequency f_{RH} (> f_T).

expected that the maximum LHCP gain for the C-metacurl antenna will be increased and balanced with the maximum RHCP gain.

Based on the abovementioned inference and expectation, we investigate the gain for a modified C-metacurl antenna, where some C-type metaatoms for the original C-metacurl antenna in Fig. 5 are replaced by the N-type metaatoms, as shown in Fig. 10. The replacement starts from point T in Fig. 10(a) and point F in Fig.10 (b). The metacurl antennas in Fig. 10(a) and Fig. 10(b) are called the *Compound-T* and *Compound-F metacurl antennas*, respectively.

FIGURE 11. Frequency response of the gain for the compound metacurl antennas with the number of N-type metaatoms as a parameter. (a) Compound-T metacurl antenna. (b) Compound-F metacurl antenna.

FIGURE 12. Radiation pattern for the compound-T metacurl antenna, where the number of N-metaatoms is $N_N = 15$. Other parameters are shown in Table 1. (a) At 2.7 GHz $\approx f_{LH}$. (b) At 3.45 GHz $\approx f_{RH}$. Note that the radiation pattern is normalized to the maximum value at 2.7 GHz.

FIGURE 13. Frequency response of the VSWR for the compound-T metacurl antenna, where the number of N-type metaatoms is $N_N = 15$. Other parameters are shown in Table 1. The shaded regions show LHCP and RHCP gain bandwidths.

V. FABRICATION OF THE COMPOUND-T METACURL ANTENNA AND EXPERIMENTAL RESULTS

To confirm the validity of the numerical analysis results shown in Section IV, the compound-T metacurl antenna is fabricated as shown in Fig. 14, where fifteen N-type metaatoms are used. Other parameters are shown in Table 1. Fig. 15 shows the measured frequency response of the gain. The validity of the numerical analysis is demonstrated by the reasonable agreement with the measured results. The small difference in the analysis and measured results is due to the discrepancy between the analysis values and practical values (used for the measurement) for chip capacitors and inductors.

A difference of approximately 3 dB in the maximum LHCP gain and RHCP gain for the original C-metacurl antenna discussed in Section III is reduced; both maximum gains are almost the same, with a value of approximately 7 dBi. It is found that the 3-dB gain bandwidth is 9% for the LHCP
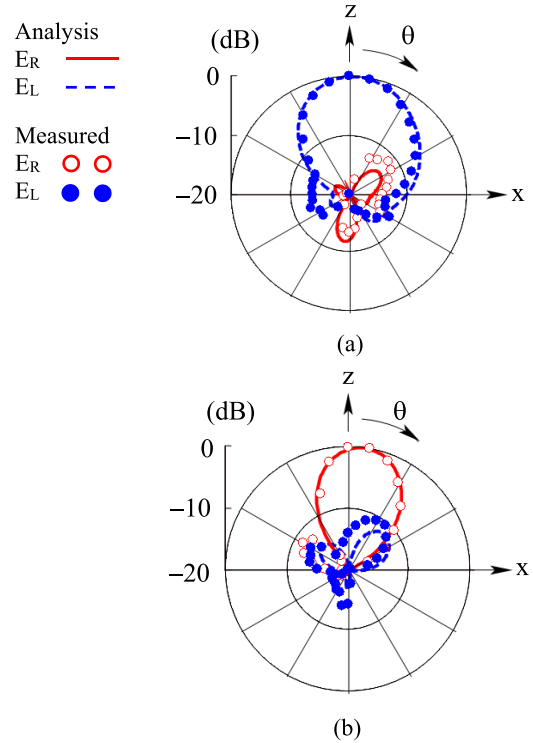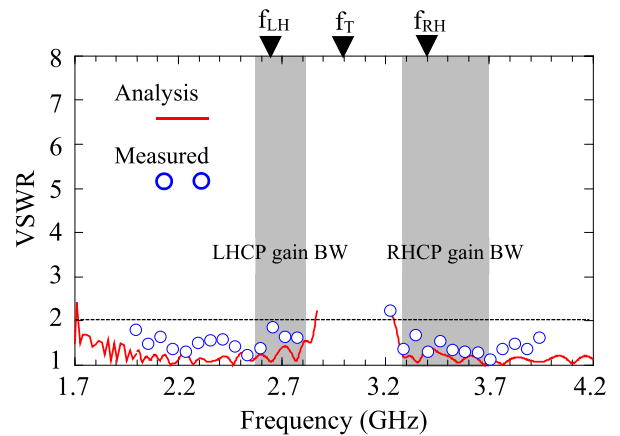
gain around f_{LH} (= 2.65 GHz) and 12% for the RHCP gain around f_{RH} (= 3.4 GHz). The difference in the 3-dB gain bandwidths is due to the difference in the gradients of the dispersion curve at f_{LH} and f_{RH} in Fig. 4. The gradient of the dispersion curve $[|\Delta\lambda_g|/\Delta f]$ at f_{RH} is smaller than that at f_{LH}, i.e., $[|\Delta\lambda_g|/\Delta f]$ at f_{RH} < $[\Delta\lambda_g/\Delta f]$ at f_{LH}. If $|\Delta\lambda_g|$ at f_{RH} and $\Delta\lambda_g$ at f_{LH} are the same values, then Δf at f_{RH} becomes wider, compared with Δf at f_{LH}. This makes the 3-dB gain
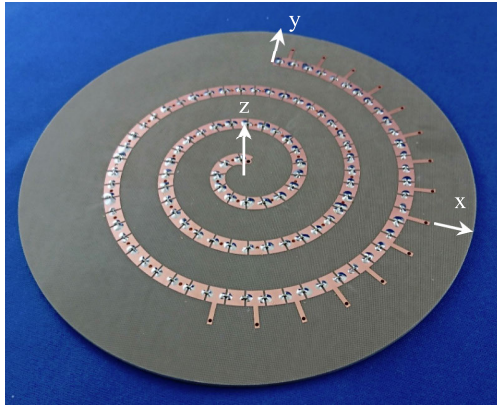
FIGURE 14. Fabricated compound-T metacurl antenna, where the number of N-type metaatoms is $N_N = 15$. Other parameters are shown in Table 1.
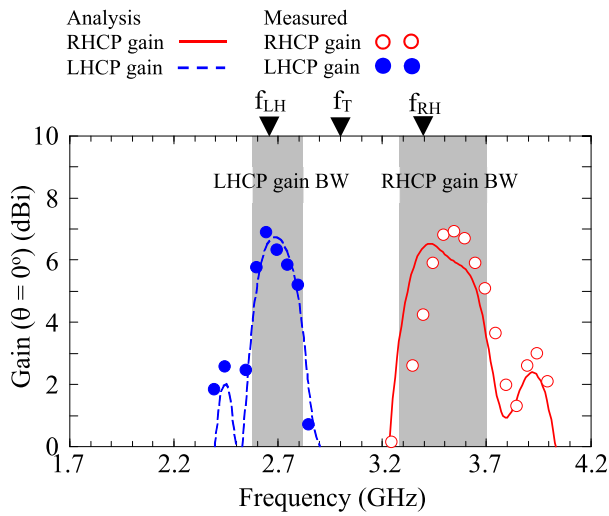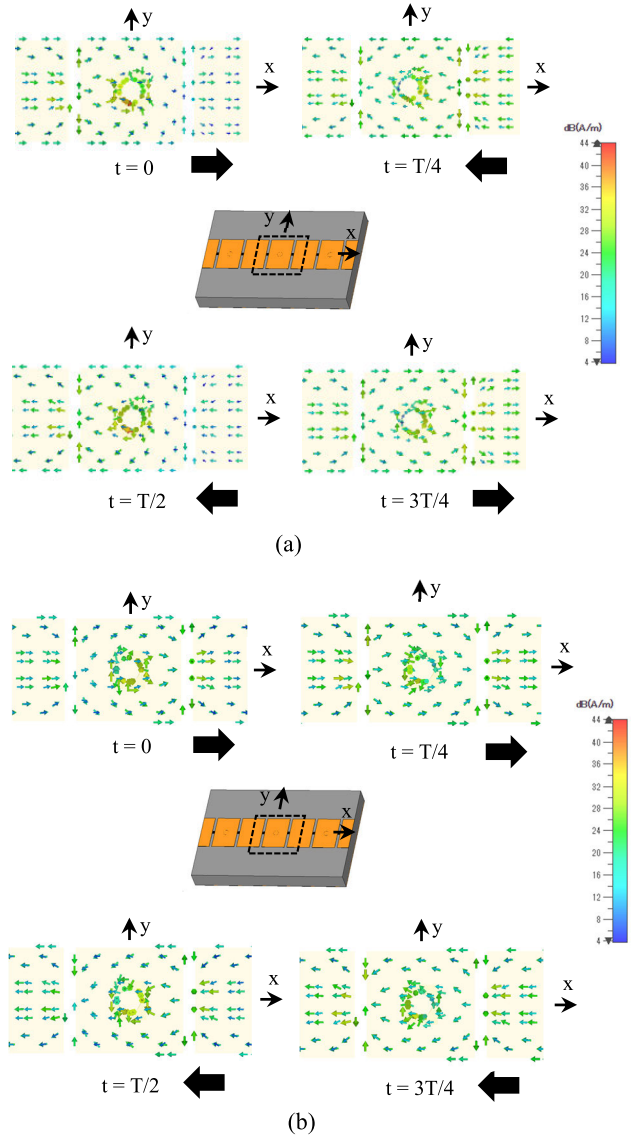

FIGURE 15. Frequency response of the gain for the fabricated compound-T metacurl antenna, where the number of N-type metaatoms is $N_N = 15$. Other parameters are shown in Table 1. The shaded regions show LHCP and RHCP gain bandwidths.

FIGURE 16. Magnetic field vectors above the surface of the C-type metaatom when time t is changed with periodicity T. (a) At frequency f_{LH} ($< f_T$). (b) At frequency f_{RH} ($> f_T$).

bandwidth for the RHCP gain wider than that for the LHCP gain.

The measured radiation pattern for the compound-T metacurl antenna is added to the analysis results in Fig. 12. Agreement of the measured radiation pattern with the numerical analysis is obtained. The LHCP wave is dominant at 2.7 GHz ≈ f_{LH}, and the RHCP wave is dominant at 3.45 GHz ≈ f_{RH}. The small cross polarized component leads to good axial ratios (ARs); analysis result is AR = 1.2 dB at 2.7 GHz (experimental results: 1.0 dB) and AR = 2.0 dB at 3.45 GHz (experimental results: 3.2 dB). The analytical AR is less than 3 dB in the LHCP and RHCP gain bandwidths.

The validity of the numerical analysis results is also found with the measured VSWR for the compound-T metacurl antenna. The measured result is added to Fig. 13. It is found that the measured VSWR across both the LHCP and RHCP gain bandwidths is small, with a value of less than 2, as desired for practical usage.

VI. CONCLUSION

Analysis has revealed that a low-profile metacurl antenna composed of C-type metaatoms has a maximum LHCP gain that is smaller than the maximum RHCP gain. Also, analysis has revealed that, as opposed to the C-type metaatom, an N-type metaatom radiates an LHCP wave. This leads to the expectation that the smaller maximum LHCP gain for the C-metacurl antenna can be increased by replacing some C-type metaatoms with N-type metaatoms. A novel antenna created by the replacement with N-type metaatoms is called the compound metacurl antenna.

Two compound metacurl antennas have been investigated: compound-T and compound-F metacurl antennas. In the compound-T metacurl antenna, the C-type metaatoms are replaced by N-type metaatoms from the arm end point T. In the compound-F metacurl antenna, replacement by

(a)

(b)
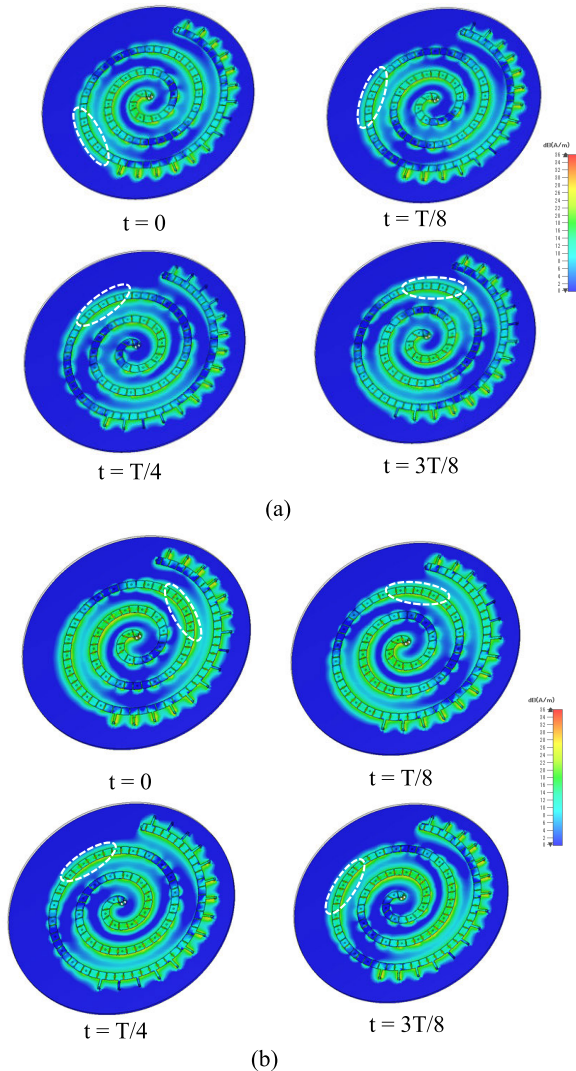
FIGURE 17. Magnetic fields above the compound-T metacurl antenna when time *t* is changed with periodicity *T*. (a) At frequency f_{LH} (< f_T). (b) At frequency f_{RH} (> f_T).

N-type metaatoms starts from point F. Analysis reveals that the maximum LHCP gain for the compound-T and compound-F metacurl antennas is increased and equals the maximum RHCP gain, when the number of N-type metaatoms is appropriately chosen.

The compound-T metacurl is fabricated and experimental work is performed to validate the analysis results. It is confirmed that the maximum LHCP gain is almost equal to the maximum RHCP gain. Other measured results, including the radiation pattern and VSWR, also show good agreement with the analysis results.

APPENDIX
A. MAGNETIC FIELD VECTORS ABOVE C-TYPE METAATOM
Compared with Fig. 9, Fig. 16 shows the change in the magnetic field vector above the C-type metaatom surface when time *t* is changed, where the frequency is fixed to be f_{LH} (= 2.65 GHz) in Fig. 16(a) and f_{RH} (= 3.4 GHz)
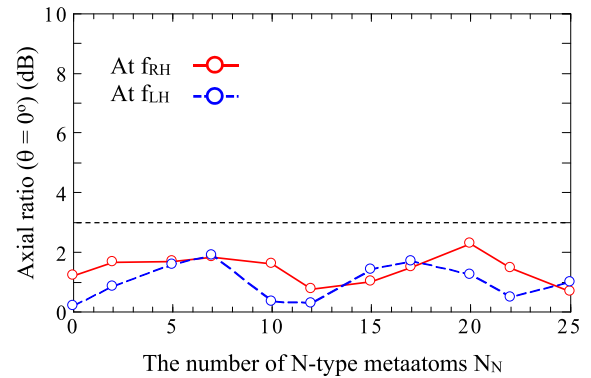
FIGURE 18. Axial ratio for the compound-T metacurl antenna as a function of the number of N-type metaatoms, N_N.

in Fig. 16(b). The magnetic field vectors are linearly changed in the x-direction at the two frequencies. This fact shows that the C-type metaatom radiates a linearly polarized wave at both frequencies.

B. MAGNETIC FIELDS ABOVE COMPOUND-T METACURL ANTENNA
Fig. 17 shows the magnetic fields above the compound-T metacurl antenna when time *t* is changed, where the frequency is fixed to be f_{LH} (= 2.65 GHz) in Fig. 17(a) and f_{RH} (= 3.4 GHz) in Fig. 17(b). The white section rotates clockwise in Fig. 17(a) and counterclockwise in Fig. 17(b).

C. EFFECTS OF THE NUMBER OF N-TYPE METAATOMS ON THE AXIAL RATIO
The axial ratios for the compound-T metacurl antenna as a function of the number of N-type metaatoms, N_N, at f_{LH} and f_{RH} are shown in Fig. 18. The effect of the number of N-type metaatoms on the axial ratio is small and the axial ratio is less than 3 dB.

REFERENCES
[1] J. D. Kraus, "Helical beam antenna," *Electronics*, vol. 20, pp. 109–111, Apr. 1947.
[2] J. D. Kraus, "Helical beam antennas for wide-band applications," *Proc. IRE*, vol. 36, no. 10, pp. 1236–1242, Oct. 1948.
[3] J. D. Kraus and R. J. Marhefka, *Antennas*, 3rd ed. New York, NY, USA: McGraw-Hill, 2002, ch. 8.
[4] H. Nakano and J. Yamauchi, "Balanced feed axial mode helical antenna (I)," *IECE Jpn.*, vols. AP-78–19, pp. 23–28, Jun. 1978.
[5] H. Nakano and J. Yamauchi, "The balanced helices radiating in the axial mode," in *Proc. Antennas Propag. Soc. Int. Symp.*, Seattle, WA, USA, vol. 17, Jun. 1979, pp. 404–407.
[6] H. Nakano, *Low-profile Natural and Metamaterial Antennas: Analysis Methods and Applications*. Hoboken, NJ, USA: Wiley, 2016.
[7] R. F. Harrington, *Field Computation by Moment Methods*. New York, NY, USA: Macmillan, 1968.
[8] A. F. Peterson, S. L. Ray, and R. Mittra, *Computational Methods for Electromagnetics*. Piscataway, NJ, USA: IEEE Press, 1998.

[9] J. Kaiser, "The archimedean two-wire spiral antenna," *IRE Trans. Antennas Propag.*, vol. 8, no. 3, pp. 312–323, May 1960.

[10] W. L. Stutzman and G. A. Thiele, *Antenna Theory and Design*. Hoboken, NJ, USA: Wiley, 1981.

[11] E. Wolff, *Antenna Analysis*, Norwood, MA, USA: Artech House, 1988.

[12] J. Volakis, *Antenna Engineering Handbook*. London, U.K.: McGraw-Hill, 2007.

[13] E. S. Sakomura, D. B. Ferreira, I. Bianchi, and D. C. Nascimento, "Analysis of archimedean spiral antenna fed by hecken and exponential microstrip baluns," in *Proc. IEEE Int. Symp. Antennas Propag. USNC/URSI Nat. Radio Sci. Meeting*, Boston, MA, USA, Jul. 2018, pp. 851–852.

[14] H. Nakano and J. Yamauchi, "A theoretical investigation of the two-wire round spiral antenna," in *Proc. IEEE AP-S Int. Symp.*, Seattle, WA, USA, Jun. 1979, pp. 387–390.

[15] H. Nakano, S. Okuzawa, K. Ohishi, H. Mimaki, and J. Yamauchi, "A curl antenna," *IEEE Trans. Antennas Propag.*, vol. 41, no. 11, pp. 1570–1575, Nov. 1993.

[16] F. Yang and Y. Rahmat-Samii, "A low-profile circularly polarized curl antenna over an electromagnetic bandgap (EBG) surface," *Microw. Opt. Technol. Lett.*, vol. 31, no. 4, pp. 264–267, Nov. 2001.

[17] C. Zhang, J. Shi, and Q. Cao, "A low-profile curl antenna with parasitic curl," in *Proc. IEEE 5th Asia–Pacific Conf. Antennas Propag. (APCAP)*, Kaohsiung City, Taiwan, Jul. 2016, pp. 139–140.

[18] H. Zhou, A. Pal, A. Mehta, H. Nakano, A. Modigliana, T. Arampatzis, and P. Howland, "Reconfigurable phased array antenna consisting of high-gain high-tilt circularly polarized four-arm curl elements for near horizon scanning satellite applications," *IEEE Antennas Wireless Propag. Lett.*, vol. 17, no. 12, pp. 2324–2328, Dec. 2018.

[19] L. Shafai, "Some array applications of the curl antenna," *Electromagnetics*, vol. 20, no. 4, pp. 271–293, Jul. 2000.

[20] P. J. Massey, P. Fellows, D. Mirshekar-Syahkal, A. Pal, and A. Mehta, "Loop antennas," in *Handbook of Antenna Technologies*, vol. 2. Singapore: Springer, 2016, pp. 723–786.

[21] C. Balanis, *Antennas Theory*. Hoboken, NJ, USA: Wiley, 2005, ch. 5.

[22] H. Nakano, "A numerical approach to line antennas printed on dielectric materials," *Comput. Phys. Commun.*, vol. 68, nos. 1–3, pp. 441–450, Nov. 1991.

[23] H. Nakano, Y. Okuyama, J. Miyake, and J. Yamauchi, "Counter circularly-polarized curl antenna with a lossy structure," in *Proc. IEEE Antennas Propag. Soc. Int. Symp. (APSURSI)*, Orlando, FL, USA, Jul. 2013, pp. 154–155.

[24] C. Caloz and T. Itoh, *Electromagnetic Metamaterials*, Hoboken, NJ, USA: Wiley, 2006.

[25] G. Eleftheriades and K. Balmain, *Negative-Refraction Metamaterials: Fundamental Principles and Applications*. New York, NY, USA: Wiley, 2005.

[26] N. Engheta and R. W. Ziolkowski, *Electromagnetic Metamaterials: Physics and Engineering Explorations*. New York, NY, USA: Wiley, 2006.

[27] H. Nakano, J. Miyake, T. Sakurada, and J. Yamauchi, "Dual-band counter circularly polarized radiation from a single-arm metamaterial-based spiral antenna," *IEEE Trans. Antennas Propag.*, vol. 61, no. 6, pp. 2938–2947, Jun. 2013.

[28] H. Nakano, I. Yoshino, T. Abe, and J. Yamauchi, "Balanced gain for a square metaloop antenna," *EPJ Appl. Metamaterials*, vol. 6, p. 3, Aug. 2019.

[29] CST Computer Simulation Technology GmbH, Darmstadt, Germany. *Microwave Studio*. Accessed: Jan. 2020. [Online]. Available: http://www.cst.com

HISAMATSU NAKANO (Life Fellow, IEEE) has been with Hosei University, since 1973, where he is currently a Professor Emeritus and a special-appointment Researcher with the Electromagnetic Wave Engineering Research Institute attached to the graduate school. He has held positions, such as a Visiting Associate Professor at Syracuse University, from March 1981 to September 1981, and a Visiting Professor at the University of Manitoba, from March 1986 to September 1986, University of California, Los Angeles, from September 1986 to March 1987, and Swansea University, U.K., from July 2016 to September 2019. He has published over 330 articles in peer-reviewed journals and 11 books/book-chapters, including *Low-profile Natural and Metamaterial Antennas* (IEEE Press, Wiley, 2016). His significant contributions are the development of five integral equations for line antennas and the realization of numerous wideband antennas, including curl, spiral, helical, and cross-wire antennas. His other accomplishments include antennas for GPS, personal handy phone, space radio, electronic toll collection, RFID, UWB, and radar. He has been awarded 78 patents, including A Curl Antenna Element and Its Array, Japan. His research topics include numerical methods for low- and high-frequency antennas and optical waveguides. He served as a member of the IEEE APS Administrative Committee, from 2000 to 2002, and a Region 10 Representative, from 2001 to 2010. He received the H. A. Wheeler Award, in 1994, the Chen-To Tai Distinguished Educator Award, in 2006, and the Distinguished Achievement Award, in 2016, all from the IEEE Antennas and Propagation Society. He was also a recipient of The Prize for Science and Technology from Japan's Minister of Education, Culture, Sports, Science and Technology, in 2010. He is an Associate Editor of several journals and magazines, such as *Electromagnetics* and the *IEEE Antennas and Propagation Magazine*.
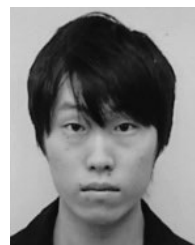
TOMOKI ABE (Member, IEEE) was born in Miyagi, Japan, in August 1994. He received the B.E. and M.E. degrees in electronics and electrical engineering from Hosei University, Tokyo, Japan, in 2017 and 2019, respectively. He is a member of the Institute of Electronics, Information and Communication Engineers of Japan.

AMIT MEHTA (Senior Member, IEEE) received the B.Eng. degree in electronics and telecommunication from the University of Pune, India, and the M.Sc. degree in telecommunications and information networks and the Ph.D. degree in smart reconfigurable antennas from the University of Essex, U.K. He is currently with the Director of the RF Research Group, Swansea University, U.K., where his core research interests are wireless communications, and microwave systems and antennas. He is leading large projects teams on 5G, adaptive antennas for GNSS, high throughput satellite communications, IOT, and milli-meter waves. He has successfully supervised over 20 post graduate research theses. He has over 100 technical publications. He holds three patents on the invention of the steerable beam smart antennas and concealed weapons detection systems.

JUNJI YAMAUCHI (Life Fellow, IEEE) was born in Nagoya, Japan, in August 1953. He received the B.E., M.E., and Dr.E. degrees from Hosei University, Tokyo, Japan, in 1976, 1978, and 1982, respectively. From 1984 to 1988, he served as a Lecturer with the Electrical Engineering Department, Tokyo Metropolitan Technical College. Since 1988, he has been a member of the faculty of Hosei University, where he is currently a Professor with the Electrical and Electronic Engineering Department. He is the author of *Propagating Beam Analysis of Optical Waveguides* (Research Studies Press, 2003). His research interests include optical waveguides, polarization converters, and circularly polarized antennas. He is a member of the Optical Society of America and the Institute of Electronics, Information and Communication Engineers of Japan.

• • •